Molecular interactions and inhibition of the staphylococcal biofilm-forming protein SdrC

Cécile Feuillie[a,1], Cécile Formosa-Dague[a,1], Leanne M. C. Hays[b,1], Ophélie Vervaeck[a], Sylvie Derclaye[a], Marian P. Brennan[c], Timothy J. Foster[b], Joan A. Geoghegan[b,2], and Yves F. Dufrêne[a,d,2]

[a]Institute of Life Sciences, Université Catholique de Louvain, B-1348 Louvain-la-Neuve, Belgium; [b]Department of Microbiology, Moyne Institute of Preventive Medicine, School of Genetics and Microbiology, Trinity College Dublin, Dublin 2, Ireland; [c]Molecular and Cellular Therapeutics, Irish Centre for Vascular Biology, Royal College of Surgeons in Ireland, Dublin 2, Ireland; and [d]Walloon Excellence in Life Sciences and Biotechnology (WELBIO), 1300 Wavre, Belgium

Edited by Richard P. Novick, New York University School of Medicine, New York, NY, and approved February 27, 2017 (received for review October 11, 2016)

Staphylococcus aureus **forms biofilms on indwelling medical devices using a variety of cell-surface proteins. There is growing evidence that specific homophilic interactions between these proteins represent an important mechanism of cell accumulation during biofilm formation, but the underlying molecular mechanisms are still not well-understood. Here we report the direct measurement of homophilic binding forces by the serine-aspartate repeat protein SdrC and their inhibition by a peptide. Using single-cell and single-molecule force measurements, we find that SdrC is engaged in low-affinity homophilic bonds that promote cell–cell adhesion. Low-affinity intercellular adhesion may play a role in favoring biofilm dynamics. We show that SdrC also mediates strong cellular interactions with hydrophobic surfaces, which are likely to be involved in the initial attachment to biomaterials, the first stage of biofilm formation. Furthermore, we demonstrate that a peptide derived from β-neurexin is a powerful competitive inhibitor capable of efficiently blocking surface attachment, homophilic adhesion, and biofilm accumulation. Molecular modeling suggests that this blocking activity may originate from binding of the peptide to a sequence of SdrC involved in homophilic interactions. Our study opens up avenues for understanding the role of homophilic interactions in staphylococcal adhesion, and for the design of new molecules to prevent biofilm formation during infection.**

Staphylococcus aureus | SdrC | adhesion | biofilms | inhibition

The nosocomial pathogen *Staphylococcus aureus* is a major cause of superficial and invasive infections. A remarkable trait of this bacterium is its ability to form biofilms on implanted devices, thereby triggering infections that are difficult to treat with antibiotics (1, 2). Biofilm formation is initiated by attachment of the bacteria to abiotic surfaces, protein-coated materials, and host cells, and followed by cell–cell adhesion and multiplication leading to a mature biofilm (1, 2). A variety of cell-surface components are involved in intercellular interactions (2, 3). Although the polycationic polysaccharide intercellular adhesin has long been thought to be the main component promoting intercellular adhesion (4, 5), there is now a compelling body of evidence that cell wall-anchored (CWA) proteins are also involved (2, 3). Several recombinant CWA proteins have been shown to form dimers in solution (6–9). In some cases (i.e., Aap), crystallographic studies have provided insights into the mechanism of dimer formation (9, 10). Although very useful, in vitro methods provide information on purified molecules that are removed from their cellular context. Clearly, elucidating the molecular mechanisms by which CWA proteins self-associate in vivo is key to enhancing our understanding of biofilm accumulation.

The increase of multidrug-resistant strains has created an urgent need for new therapeutics for bacterial infections. Biofilm inhibitors, where bacteria are prevented from forming biofilms rather than being killed, are an alternative to antibiotics (11, 12). An exciting approach is to competitively block intercellular adhesion, for example with antibodies or peptides that bind to CWA proteins and prevent homophilic interactions. The design of effective antibiofilm strategies against staphylococcal infections will depend on the identification of new inhibitory molecules and new targets but also on the availability of innovative techniques for the rapid quantification of antibiofilm activity.

Single-cell technologies enable researchers to probe individual microbial cells, rather than cell populations, thereby providing a means to better understand cellular heterogeneity and interactions (13). Among these new tools, atomic force microscopy (AFM) allows us to analyze the organization, biophysical properties, and interactions of cell-wall molecules directly in single cells (14, 15). During the past years, there has been much progress in applying AFM techniques to explore the forces involved in cell adhesion and biofilm formation by staphylococci, down to molecular resolution (16–23). Here, we used AFM to study the forces guiding the self-association of the *S. aureus* serine-aspartate repeat protein SdrC (Fig. 1*A*). Phage display screening showed that the N2 subdomain mediates SdrC–SdrC interactions (24). Purified phage clones expressing a combination of two sequences from the N2 subdomain, $RPGSV_{247–251}$ and $VDQYT_{288–292}$, completely inhibited the self-association (dimerization) of SdrC proteins (24). With this in mind, we measured the strength and dynamics of the SdrC homophilic interaction, using both bacterial cells expressing full-length SdrC

Significance

The bacterial pathogen *Staphylococcus aureus* shows a remarkable ability to aggregate, thereby contributing to the formation of cellular communities that are difficult to eradicate. In this study, we dissect the homophilic interactions at play during *S. aureus* cell–cell adhesion, focusing on the key surface protein SdrC. We discover that SdrC is engaged in low-affinity homophilic bonds that promote intercellular adhesion, and that it also favors strong hydrophobic interactions with surfaces, emphasizing that this protein is a multifunctional adhesin. We also show that SdrC-dependent cell-surface attachment, cell–cell adhesion, and biofilm formation can be efficiently blocked by a peptide, thus suggesting this approach could be used for antibiofilm therapy.

Author contributions: C.F., C.F.-D., L.M.C.H., O.V., S.D., M.B., T.J.F., J.A.G., and Y.F.D. designed research; C.F., C.F.-D., L.M.C.H., O.V., and S.D. performed research; C.F., C.F.-D., L.M.C.H., O.V., S.D., M.B., T.J.F., J.A.G., and Y.F.D. analyzed data; and C.F., C.F.-D., L.M.C.H., O.V., S.D., M.B., T.J.F., J.A.G., and Y.F.D. wrote the paper.

The authors declare no conflict of interest.

This article is a PNAS Direct Submission.

Freely available online through the PNAS open access option.

[1]C.F., C.F.-D., and L.M.C.H. contributed equally to his work.

[2]To whom correspondence may be addressed. Email: geoghegj@tcd.ie or yves.dufrene@uclouvain.be.

This article contains supporting information online at www.pnas.org/lookup/suppl/doi:10.1073/pnas.1616805114/-/DCSupplemental.

www.pnas.org/cgi/doi/10.1073/pnas.1616805114

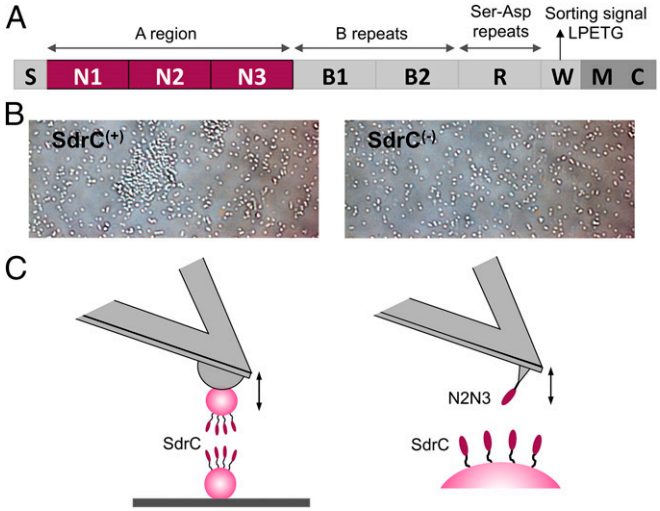

Fig. 1. Probing SdrC homophilic adhesion from the micro- to the nanoscale. (*A*) Schematic representation of the SdrC structure: S, secretory signal sequence; region A comprising N1, N2, and N3 subdomains; two B regions; region R comprising serine-aspartate (Ser-Asp; SD) dipeptide repeats; and C-terminal region containing a sorting signal with an LPETG motif, a wall spanning region (W), membrane spanning region (M), and cytoplasmic tail (C). (*B*) Optical microscopy images of *L. lactis* cells expressing—or not—full-length SdrC [respectively, SdrC$^{(+)}$ and SdrC$^{(-)}$ cells] after resuspension in PBS. (*C*) Force spectroscopy of the SdrC homophilic interaction. (*C, Left*) We used single-cell force spectroscopy to measure the forces between *L. lactis* SdrC$^{(+)}$ bacteria expressing full-length SdrC. (*C, Right*) Single-molecule force spectroscopy was used to probe the forces between recombinant $SdrC_{N2N3}$ protein, engaged in homophilic binding, and full-length SdrC on *L. lactis*.

proteins and a recombinant polypeptide containing the N2 and N3 subdomains. To investigate SdrC interactions in the absence of other staphylococcal components, we focused on a *Lactococcus lactis* strain expressing SdrC [hereafter SdrC$^{(+)}$] (24). We also analyzed a methicillin-resistant *S. aureus* (MRSA) strain to support the biological relevance of our findings. The results show that the SdrC homophilic interaction is weak and dissociates quickly, and that the protein also promotes strong hydrophobic interaction with inert surfaces. In silico molecular modeling suggests that a peptide derived from the neuronal cell-adhesion molecule β-neurexin, a ligand for SdrC (25), binds the protein at a site that overlaps $RPGSV_{247–251}$. We demonstrate the ability of this peptide to block SdrC-dependent cell-surface attachment, cell-cell adhesion, and biofilm formation.

Results

Forces in SdrC-Mediated Intercellular Adhesion. Before AFM analysis, we confirmed the involvement of SdrC in intercellular adhesion using a microscale assay. Optical microscopy images showed that *L. lactis* SdrC$^{(+)}$ cells suspended in buffer formed aggregates, unlike *L. lactis* SdrC$^{(-)}$ cells, which were mainly isolated (Fig. 1*B*). These data show that SdrC induces intercellular adhesion (24), and that the protein is properly exposed on the cell surface.

We first investigated the strength of cell–cell adhesion by measuring the forces between individual *L. lactis* SdrC$^{(+)}$ cells using single-cell force spectroscopy (SCFS) (Fig. 1*C*, *Left*). As shown in Fig. 2 *A* and *B*, most force curves (70%, average from six cell pairs) obtained at short contact time (100 ms) between SdrC$^{(+)}$ cells showed adhesion events with a maximum adhesion force of 98 ± 26 pN and a rupture length of 160 ± 86 nm (n = 2,400 curves from six cell pairs). Mostly single well-defined adhesion events were observed, which suggests they involve the rupture of a small number of molecular bonds that rupture in parallel. Adhesion forces increased with increasing the contact time to 1 s (280 ± 113 pN; Fig. 2 *C* and *D*), indicating that cell–cell bonds strengthen with the duration of adhesion (19, 26). Force profiles showed multiple ruptures, unlike the 100-ms curves, which we believe result from the sequential rupture of multiple bonds. Adhesive interactions were not seen between SdrC$^{(-)}$ cells (Fig. 2 *E* and *F*) or between SdrC$^{(+)}$ and SdrC$^{(-)}$ cells (Fig. 2 *G* and *H*), thus demonstrating that intercellular adhesion involves SdrC homophilic bonds, that is, bonds formed between adhesins located on opposing cells, rather than protein–ligand binding.

Cell–cell separation did not lead to the complete unfolding of the SdrC protein. Considering that each amino acid contributes 0.36 nm to the contour length of a fully extended polypeptide chain (27) and that full-length SdrC is 995 amino acids in length (24, 25), the length of two fully extended proteins is expected to be 716 nm. This is much longer than the rupture lengths we observed (~160 nm at 100 ms), thus implying that intercellular bonds rupture before complete unfolding of the proteins. Along the same line, the structurally similar serine-aspartate repeat protein G (SdrG) and fibronectin binding protein A (FnBPA) were not completely unfolded under force, reflecting a high mechanical stability (19, 20).

Occasionally, some cell pairs displayed sawtooth patterns with periodic peaks and long extensions (Fig. S1). The peak-to-peak distance was 25 ± 3 nm (n = 74 curves, 900 peaks) in most profiles (Fig. S1*B*). Neither the number of domains nor their

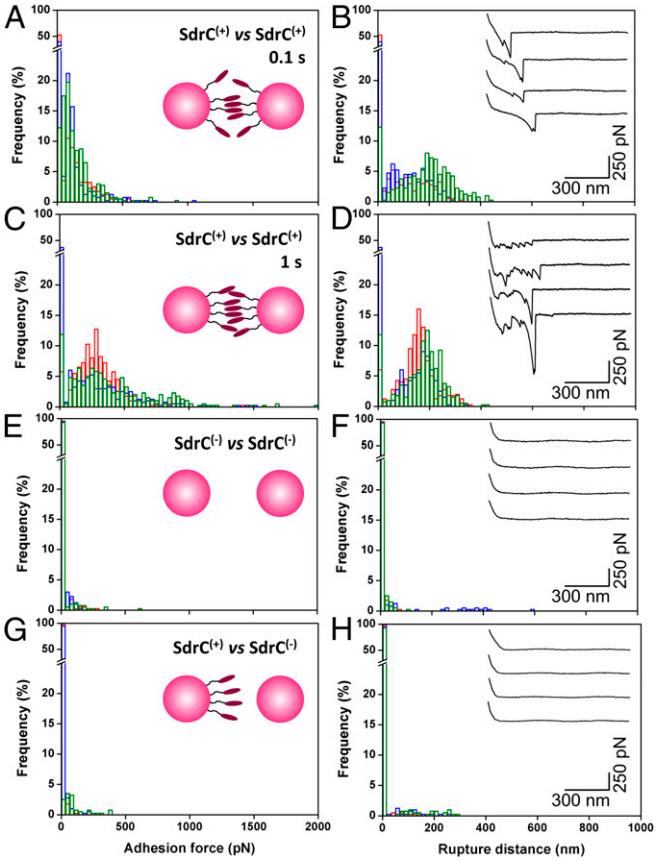

Fig. 2. Forces in cell–cell adhesion. (*A–D*) Adhesion force (*A* and *C*) and rupture distance (*B* and *D*) histograms obtained at 100 ms (*A* and *B*) or 1 s (*C* and *D*) contact time in PBS for three cell pairs (three different colors) of *L. lactis* SdrC$^{(+)}$ cells. (*E–H*) Results obtained for the interaction during 100 ms between two SdrC$^{(-)}$ cells (*E* and *F*) and between SdrC$^{(+)}$ and SdrC$^{(-)}$ cells (*G* and *H*). (*Insets*) Representative force signatures. All curves were obtained using an applied force of 250 pN and an approach and retraction speed of 1.0 μm/s.

MICROBIOLOGY

lengths match the structure of SdrC, which is made of five larger domains, namely three N subdomains comprising 132, 153, and 162 residues and two B domains of ∼104 residues. The 25-nm-length increment may result from the unfolding of the homophilic binding region of the N2 subdomain [amino acid sequences $RPGSV_{247–251}$ and $VDQYT_{288–292}$ (24)]. We propose that the periodic force peaks reflect the rupture of multiple homophilic interactions one by one, in a zipper-like fashion. The lateral assembly of SdrC on the cell surface may lead to cooperative interactions that enhance cell–cell adhesion. Such a mechanism is reminiscent of the homophilic cadherin–cadherin interaction in mammalian cells, where multiple binding contacts between opposing surfaces allow for a greater stability in cell–cell interactions (28, 29).

SdrC-Dependent Adhesion Forces in a Methicillin-Resistant *S. aureus*. Throughout this study, SdrC interactions were investigated in a model *L. lactis* strain to avoid any interference from other surface components. A pertinent question is whether these forces also contribute to biofilm accumulation by *S. aureus*. We therefore analyzed cell–cell adhesion forces in the clinically relevant MRSA252 strain. As shown in Fig. S2 *A* and *B*, MRSA252 cells at short contact time (n = 2,400 curves from six cell pairs) featured single well-defined adhesion peaks in about 8% of the curves, with a shape similar to that observed for *L. lactis* $SdrC^{(+)}$ cells. Intercellular adhesion forces were strongly reduced in MRSA252Δ*sdrC* mutant cells deficient in SdrC (Fig. S2 *E* and *F*), indicating they involve SdrC-dependent interactions. This was further confirmed by showing that biofilm formation was reduced in the MRSA252Δ*sdrC* mutant compared with the wild type (Fig. S3). In addition, forces between MRSA252 and MRSA252Δ*sdrC* cells were also much weaker (Fig. S2 *G* and *H*), implying that cell–cell adhesion in the MRSA252 strain is primarily mediated by homophilic bonds and thus that SdrC hardly binds to other staphylococcal components. Increasing the contact time increased the adhesion probability to 29% and the adhesion force to 42 ± 16 pN (Fig. S2 *C* and *D*). The adhesion force and adhesion probability were always much lower for MRSA cells than for *L. lactis* cells, consistent with the fact that *L. lactis* can accumulate more SdrC molecules on the cell surface and that there is less interference from other CWA proteins. Indeed, single-molecule experiments, discussed below, reveal that, on average, the adhesion force between MRSA252 cells corresponds to the strength of a single SdrC–SdrC bond, whereas the force between *L. lactis* cells involves two (or three) bonds. In summary, the similar SdrC-dependent forces in the MRSA and *L. lactis* strains support the validity of our model system and the biological relevance of the results.

MRSA252 cells did not show the sawtooth force profiles sometimes observed with *L. lactis* cells, which is likely to result from the lower surface density of SdrC. However, this observation does not exclude the possibility that zipper-like adhesion will occur in real *S. aureus* biofilms. First, it should be kept in mind that AFM measures the forces on localized cell–cell contacts, meaning that the probability of detecting zipper interactions will depend on the local protein density and on the complex macromolecular organization of the surface. Furthermore, cell–cell interaction times in biofilms can be much longer than in our setup (1 s), thus favoring the formation of zipper-like bonds. Finally, expression of SdrC can greatly vary depending on the strain and on environmental conditions (stage of infection, growth phase). Barbu et al. (24) found that SdrC expression is stronger during late exponential to stationary phase, and that the ability to block biofilm formation by interfering with SdrC dimerization is strain-dependent.

SdrC Mediates Strong Bacterial Attachment to Hydrophobic Surfaces. SdrC has been shown to promote bacterial adherence to plastic surfaces (24), but whether this is related to the hydrophobicity of the protein is unclear. To test the hypothesis that SdrC contributes to hydrophobic interactions with inert surfaces, we measured the forces between *L. lactis* $SdrC^{(+)}$ cells and hydrophobic, methyl-terminated substrates (Fig. 3 *A* and *B*). All curves displayed adhesion force events that were remarkably strong, ranging from 5,000 to 20,000 pN depending on the cell. SdrC largely contributed to these forces, as they were strongly reduced in *L. lactis* $SdrC^{(-)}$ cells (Fig. 3 *C* and *D*). Interestingly, rupture lengths (412 ± 12 nm, mean and SD of three cells) were close to the length of fully extended SdrC proteins (360 nm). This leads us to believe that unlike the weak cell–cell interaction, the strong cell–substrate interaction leads to the complete unfolding of SdrC. We speculate that protein unfolding will expose hydrophobic residues [SdrC contains 21% hydrophobic amino acids (24)], thereby strengthening hydrophobic attachment to surfaces. As the unfolding force of cellular proteins is typically ∼200 to 250 pN (27), the large adhesion forces may involve up to ∼100 adhesins, consistent with their high surface concentration. We also studied bacterial interactions with hydrophilic, hydroxyl-terminated surfaces (Fig. S4). Much weaker forces were measured, showing that the strong adhesion forces mostly originate from hydrophobic bonds. Shorter extensions were also observed, which implies that the proteins were not (or only partially) unfolded. Collectively, these findings demonstrate that SdrC enables strong hydrophobic interactions with abiotic surfaces, which are of biological relevance, as we expect them to play a role in the colonization of inert materials, the first stage of biofilm formation. This emphasizes the idea that the protein is a multifunctional adhesin implicated in bacterial adherence to inert surfaces and in cell–cell adhesion.

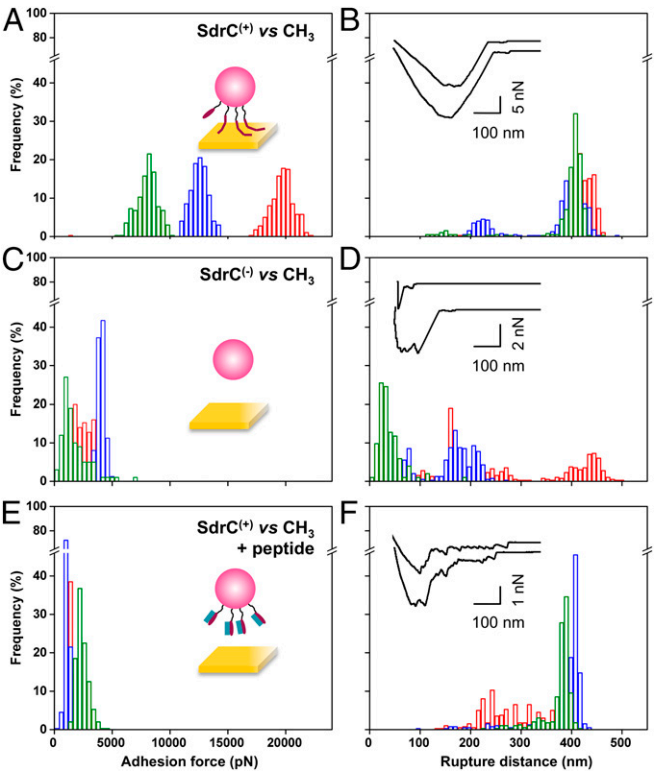

Fig. 3. Forces guiding bacterial attachment to hydrophobic surfaces. (*A–D*) Adhesion force (*A* and *C*) and rupture distance (*B* and *D*) histograms obtained in PBS between three different *L. lactis* $SdrC^{(+)}$ cells (*A* and *B*) or *L. lactis* $SdrC^{(-)}$ cells (*C* and *D*) and hydrophobic, methyl-terminated substrates. (*E* and *F*) Force data collected for *L. lactis* $SdrC^{(+)}$ cells in the presence of β-neurexin–derived peptide (2 μM). (*Insets*) Representative force signatures. Curves were obtained using a contact time of 100 ms, an applied force of 250 pN, and an approach and retraction speed of 1.0 μm/s.

Molecular Details of the SdrC Homophilic Bond. We then studied the strength and affinity of single SdrC–SdrC bonds, by measuring the forces between recombinant $SdrC_{N2N3}$ attached to AFM tips and full-length SdrC proteins on $SdrC^{(+)}$ cells (Fig. 4*A*). A substantial fraction (~28%, from 13 cells) of the force curves recorded across the cell surface featured single well-defined adhesion peaks. These forces were not detected on $SdrC^{(-)}$ cells (Fig. 4*B*), thus showing that they reflect specific SdrC–SdrC bonds. The adhesion force histogram revealed a multimodal distribution with a main maximum at 36 ± 16 pN (from 13 cells from 10 independent cultures) followed by smaller maxima at ~80, ~120, and ~160 pN. This force distribution strongly suggests that the ~40-pN binding force corresponds to the interaction strength quantum between two SdrC N2N3 domains, whereas the larger forces would reflect the rupture of multiple interactions in parallel. This is directly supported by the fact that the ~40-pN unit force matches the mean interaction force measured between two *S. aureus* MRSA252 cells (Fig. S2). Presumably, the ~100-pN forces measured between *L. lactis* $SdrC^{(+)}$ cells involve two or three interacting pairs of SdrC proteins. Our ~40-pN force is much weaker than the ~2-nN force measured for SdrG–fibrinogen bonds (19), indicating that SdrC homophilic adhesion does not involve a high-affinity binding mechanism. However, such moderate binding strength is in the range of that measured by AFM for cadherin homophilic bonds (30).

We next studied the affinity of the homophilic bond by measuring the dynamics of the interaction. To estimate the dissociation rate, we recorded force curves at various loading rates on six cells from four independent cultures (Fig. 4*C*). To account for the contribution of cell elasticity, the effective loading rate was estimated from the force-versus-time curves (31). Fig. 4*C* shows that the mean adhesion force (F) increased linearly with the logarithm of the loading rate (r), as observed earlier for homophilic complexes (20, 30, 32, 33). Using the slope (f_β) of the F-versus-ln(r) plot, we estimated the length scale of the energy barrier, x_β = 0.5 nm. The kinetic off-rate constant of dissociation at zero force was obtained by extrapolation to zero force, $k_{off} = r_{F=0}x_\beta/k_BT$ = 0.4 s^{-1}. This fast off-rate, close to that of homophilic cadherin and FnBPA bonds (20, 30), means that the bond dissociates rapidly, and thus that homophilic adhesion is a dynamic process.

We also estimated the association rate by varying the interaction time while keeping the loading rate constant. The adhesion frequency (i.e., number of curves with adhesion events) increased quickly to reach a plateau corresponding to almost 100% after 1 s (Fig. 4*D*; data from five cells from five independent cultures). Such a fast bond formation was also reported for cadherins (20, 30). Considering the interaction time needed for half-maximal probability of binding, $t_{0.5}$ = 240 ms, the association rate constant can be estimated: $k_{on} = {t_{0.5}}^{-1}N_AV_{eff}$ = 2,690 $M^{-1}{\cdot}s^{-1}$, where V_{eff} is the effective volume explored by the tip-tethered protein (approximated here to a half-sphere of radius r_{eff} = 8 nm). From this, we deduced the equilibrium dissociation constant: $K_D = k_{off}/k_{on}$ = 160 μM. We note that this value should be taken as an estimate, as the volume explored by the probing tip is not precisely known. In our calculation, we considered that this volume is defined by the length of the N2N3 domain, ~8 nm. If extreme values for r_{eff} are considered (6 and 10 nm), the resulting K_D lies within the limits of 80 to 390 μM. These values are clearly higher than that for high-affinity bonds such as the SdrG–fibrinogen interaction [0.3 μM (19, 34)], and thus mean that the homophilic SdrC bond has a much lower affinity. Intriguingly, our dissociation constant is also greater than that estimated recently for SdrC dimerization using a solid-phase binding assay [0.3 μM (24)]. This discrepancy may reflect limitations of in vitro methods, namely that they require protein expression and purification, and involve protein labeling with biotin and further reaction with avidin probes. By contrast, AFM directly analyzes fully functional proteins on live cells, thus without purification or labeling.

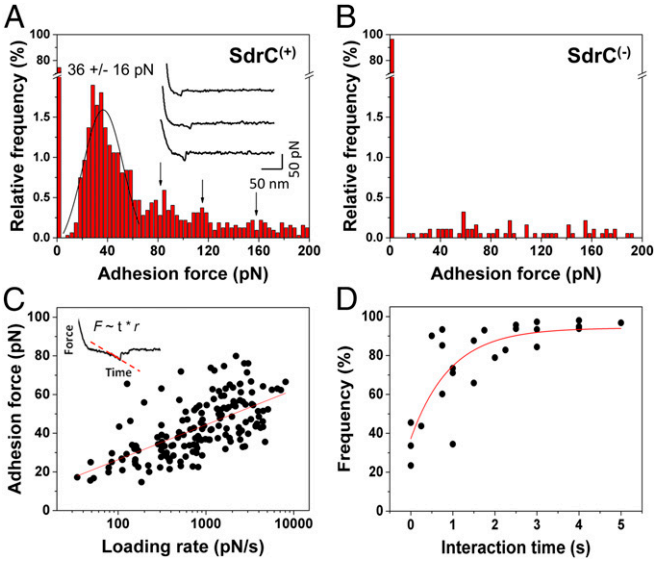

Fig. 4. Strength and dynamics of the SdrC homophilic interaction. (*A*) Adhesion forces together with representative curves (*Inset*) obtained in PBS between 13 different *L. lactis* $SdrC^{(+)}$ cells and AFM tips labeled with the recombinant $SdrC_{N2N3}$ protein. Curves were obtained using a contact time of 100 ms, an applied force of 250 pN, and an approach and retraction speed of 1.0 μm/s. (*B*) Control experiments on $SdrC^{(-)}$ cells showing the specificity of the SdrC–SdrC forces. (*C*) Dependence of the adhesion force on the loading rate applied during retraction, measured on six different cells from four independent cultures, using a contact time of 100 ms. The mean adhesion force, F, increased linearly with the logarithm of the loading rate (r): $F = 7.84\ 10^{-12}\ \ln(r) + 2.07\ 10^{-10}$. (*C*, *Inset*) Force-vs.-time curve, which was used to estimate the effective loading rate. (*D*) Dependence of the adhesion frequency on the interaction time, measured at a constant approach and retraction speed of 1.0 μm/s on five different cells from five independent cultures.

A Peptide That Strongly Blocks SdrC-Dependent Adhesion and Biofilm Formation. Phage display screening combined with biochemical and cell biology experiments showed that a peptide derived from the host protein β-neurexin is a ligand for SdrC and that ligand binding involves the N2N3 subdomains of SdrC (25). We used in silico methods to generate a molecular model of SdrC N2N3 subdomains based on the crystal structure of the closely related CWA protein Clumping factor A (ClfA). ClfA and SdrC are members of the microbial surface components recognizing adhesive matrix molecules (MSCRAMM) family of CWA proteins of staphylococci, and the crystal structures of six MSCRAMM N2N3 domains solved to date have shown that all adopt a highly similar, characteristic 3D fold (2). Molecular docking experiments were carried out to determine a likely binding site for the β-neurexin–derived peptide (SLGAHHIHHFHGSSKHHS) on the structural model of SdrC (Fig. 5*A* and Movie S1). The model suggests that the peptide binds at a site overlapping $RPGSV_{247–251}$, making contact with residues R247, G249, S250, and V251, leading us to postulate that it may interfere with homophilic interactions.

To test this hypothesis, we assessed the ability of the peptide to interfere with cell–cell adhesion forces, using SCFS. In Fig. 5*B*, we present the probability of cell–cell adhesion forces measured upon addition of peptide at increasing concentrations for several cell pairs. From these concentration-dependent plots, we estimate that the concentration required to inhibit 50% of maximum binding, IC_{50}, is in the range of ~0.5 to 1 μM. The adhesion probability was not altered by addition of a scrambled peptide. In summary, our analyses show that the β-neurexin peptide is a strong competitive inhibitor of the SdrC homophilic interaction, a behavior that is due to its ability to bind the N2N3 domain of SdrC with high affinity (25). Interestingly, we also found that addition of

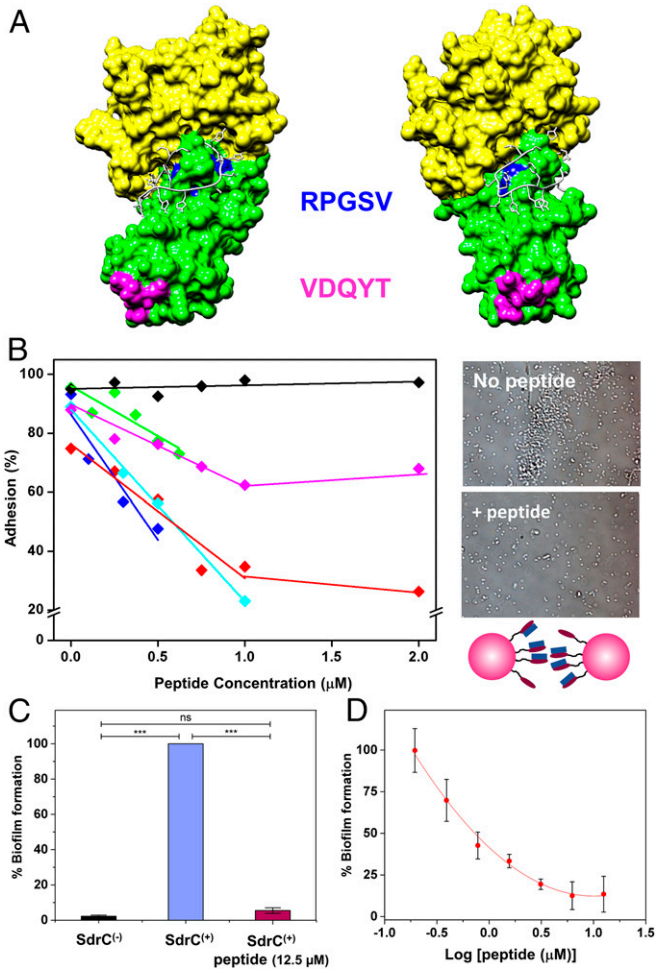

Fig. 5. Blocking cell–cell adhesion forces using β-neurexin–derived peptide. (*A*) Molecular model of the SdrC–peptide interaction. SdrC N2 and N3 subdomains are colored green and yellow, respectively. The RPGSV and VDQYT sequences are colored blue and pink, respectively. The peptide is shown in white in stick format. The image shown (*Right*) is rotated 42° compared with the view (*Left*). (*B*) Inhibition of cell–cell adhesion forces. Variation of the adhesion probability measured by SCFS for five *L. lactis* SdrC$^{(+)}$ cell pairs (different colors) upon addition of β-neurexin–derived peptide at increasing concentrations. As a control, a scrambled peptide was tested (black symbols). (*B*, *Right*) Optical images showing *L. lactis* SdrC$^{(+)}$ bacteria before and after addition of 12.5 μM peptide. (*C* and *D*) Inhibition of SdrC-mediated biofilm formation. SdrC$^{(+)}$ and SdrC$^{(-)}$ cells were allowed to form a biofilm at 30 °C for 24 h and stained with crystal violet, and the absorbance was measured at 570 nm. Values are expressed as the percentage of the value for wells containing SdrC$^{(+)}$ bacteria without peptide. Results shown are the mean values of triplicate samples, and error bars represent the SEM; *P* values were calculated using Student's *t* test. ***$P < 0.001$; ns, not significant. In *D*, varying concentrations of the peptide (0.195 to 12.5 μM) were added to the diluted bacteria before addition to the microtiter plate.

the peptide at 2 μM dramatically reduced the mean adhesion force between the cells and hydrophobic surfaces (Fig. 3 *E* and *F*).

Finally, we tested whether the peptide inhibitor could prevent SdrC-dependent biofilm formation. Biofilms formed by SdrC$^{(+)}$ bacteria were abolished in the presence of the peptide (Fig. 5*C*). The effect on biofilm formation was not due to inhibition of bacterial growth (Fig. S5). We estimated the concentration required to inhibit 50% of maximal biofilm formation, IC_{50}, as 0.9 μM (Fig. 5*D*), which is remarkably close to the value estimated for single cell–cell adhesion. We also found that the peptide is capable of inhibiting SdrC-dependent biofilm formation in the MRSA252 strain (Fig. S3), thus supporting the biological relevance of our findings. Our observation that a peptide derived from β-neurexin is a powerful competitive inhibitor capable of efficiently blocking SdrC-mediated adhesion and biofilm formation raises the possibility that this peptide could be used to prevent biofilm infections by *S. aureus*.

Discussion

Recent reports have shown that protein-mediated homophilic interactions are involved in the accumulation phase of biofilm formation by *S. aureus*, but the molecular details (i.e., strength and affinity) are not well-understood. We have studied the force and dynamics of single SdrC homophilic interactions in live cells, revealing the important role these bonds play in regulating intercellular adhesion. *L. lactis* and MRSA252 cells engage in biofilm accumulation through similar SdrC-dependent adhesion forces, supporting a major contribution of SdrC to biofilm formation by *S. aureus*. Our single-cell and single-molecule experiments are unique in that they allow us to study the binding strength and affinity of CWA proteins in their biologically relevant environment and conformation, whereas traditional methods study protein interactions after purification, and often labeling, which can alter protein functionality.

The SdrC–SdrC bond features a weak binding force (~40 pN) and low affinity (~160 μM), and involves the SdrC N2N3 subdomains. It is very likely that the N2 subdomain plays a central role, as two amino acid sequences located within N2 were previously shown to act cooperatively to promote protein dimerization (24). The fast dynamics of the SdrC interaction could be of biological significance, as it may favor cell detachment and help bacteria to disseminate and colonize new sites. The correlation between the occurrence of homophilic bonds and the level of microscale cell–cell adhesion suggests that these interactions play an important functional role in biofilm accumulation. Our observations are reminiscent of the behavior of another CWA protein, FnBPA, which promotes cell accumulation through low-affinity homophilic interactions between N2N3 domains. Biofilm formation was not fully inhibited when the *sdrC* gene was disrupted in MRSA252, which is likely due to the fact that biofilm formation in *S. aureus* is often a multifactorial process.

Interestingly, SdrC is also engaged in hydrophobic interactions with abiotic surfaces, which result from the high percentage (21%) of hydrophobic residues of the protein. SdrC-dependent hydrophobic forces are much stronger than homophilic forces, and lead to the complete unfolding of the protein upon cell-surface separation. Presumably, buried hydrophobic amino acids become exposed upon unfolding and strengthen tight attachment to the surface. We postulate that, unlike the SdrC homophilic interaction, which is weak and dissociates quickly, the strong hydrophobic interaction will favor irreversible bacterial attachment to biomaterials. Other factors contribute to the colonization of abiotic surfaces by *S. aureus*, such as teichoic acids, the autolysin Atl, and surface protein SasC (35–37). We suggest that the relative contributions of the different cell-wall components in bacterial attachment to surfaces should be revisited, paying more attention to the role of CWA proteins. Our results contribute to the accumulating evidence that SdrC is a multifunctional adhesin featuring a variety of molecular interactions that are important for regulating biofilm formation, that is, surface attachment via strong hydrophobic interactions, and cell–cell adhesion through weak homophilic bonds. In the medical context, we expect that the contribution of SdrC to biofilm formation will vary, as expression of SdrC depends on the strain and on environmental conditions (24).

Another remarkable finding of this study is a peptide that strongly inhibits SdrC-mediated cell–cell adhesion and biofilm formation. Single-cell analyses revealed that it is a powerful competitive inhibitor capable of efficiently blocking SdrC-dependent homophilic adhesion. Supporting this view, our molecular docking experiments predicted that the peptide binds to a sequence involved in homophilic interactions. The peptide used here has a sequence corresponding to a SdrC binding site at the N terminus

of human neurexin 1β. We also showed the ability of the peptide to block bacterial adhesion to inert surfaces, suggesting that the N2N3 domain of SdrC is engaged in hydrophobic interactions. The biological significance of the interaction between SdrC and neurexin 1β is unclear (25). Because the protein is only detected in neuronal tissues, it is unlikely that it acts as a ligand or inhibitor of homophilic SdrC interactions during staphylococcal biofilm infection in the bloodstream or joints. SdrC appears to be a potential target for the design of antibiofilm molecules. Live-cell nanoscopy offers promising prospects for screening peptides and small molecules capable of preventing or treating staphylococcal infections by inhibiting protein-dependent intercellular interactions.

Methods

L. lactis strain MG1363 carrying the empty plasmid pKS80 [*L. lactis* SdrC$^{(-)}$] or pKS80 with *sdrC* [*L. lactis* SdrC$^{(+)}$] (38) was grown in M17 broth supplemented with D-glucose (5 g/L; Sigma-Aldrich) and erythromycin (10 μg/mL) statically at 30 °C until stationary phase was reached. Before AFM experiments, cells were harvested by centrifugation (1,000 × *g*, 3 min) and washed two times in PBS. DNA cloning and strain construction, production of recombinant proteins, molecular modeling, aggregation and biofilm assays, and AFM methods are described in *SI Methods*.

ACKNOWLEDGMENTS. We thank David Alsteens and Philippe Herman-Bausier for help with data interpretation. Work at the Université Catholique de Louvain was supported by the European Research Council under the European Union's Horizon 2020 Research and Innovation Programme (Grant Agreement 693630), National Fund for Scientific Research (FNRS), FNRS-WELBIO (Grant WELBIO-CR-2015A-05), Federal Office for Scientific, Technical and Cultural Affairs (Interuniversity Poles of Attraction Programme), and Research Department of the Communauté Française de Belgique (Concerted Research Action). Y.F.D. and C.F.-D. are, respectively, Research Director and Postdoctoral Researcher at the FNRS. L.M.C.H. was supported by an Irish Research Council Government of Ireland Postgraduate Scholarship.

1. Otto M (2008) Staphylococcal biofilms. *Curr Top Microbiol Immunol* 322:207–228.
2. Foster TJ, Geoghegan JA, Ganesh VK, Höök M (2014) Adhesion, invasion and evasion: The many functions of the surface proteins of *Staphylococcus aureus*. *Nat Rev Microbiol* 12(1):49–62.
3. Speziale P, Pietrocola G, Foster TJ, Geoghegan JA (2014) Protein-based biofilm matrices in staphylococci. *Front Cell Infect Microbiol* 4:171.
4. Mack D, et al. (1996) The intercellular adhesin involved in biofilm accumulation of *Staphylococcus epidermidis* is a linear beta-1,6-linked glucosaminoglycan: Purification and structural analysis. *J Bacteriol* 178(1):175–183.
5. O'Gara JP (2007) ica and beyond: Biofilm mechanisms and regulation in *Staphylococcus epidermidis* and *Staphylococcus aureus*. *FEMS Microbiol Lett* 270(2):179–188.
6. Conrady DG, et al. (2008) A zinc-dependent adhesion module is responsible for intercellular adhesion in staphylococcal biofilms. *Proc Natl Acad Sci USA* 105(49): 19456–19461.
7. Geoghegan JA, et al. (2010) Role of surface protein SasG in biofilm formation by *Staphylococcus aureus*. *J Bacteriol* 192(21):5663–5673.
8. Missineo A, et al. (2014) IsdC from *Staphylococcus lugdunensis* induces biofilm formation under low-iron growth conditions. *Infect Immun* 82(6):2448–2459.
9. Yang Y-H, et al. (2014) Structural insights into SraP-mediated *Staphylococcus aureus* adhesion to host cells. *PLoS Pathog* 10(6):e1004169.
10. Conrady DG, Wilson JJ, Herr AB (2013) Structural basis for Zn^{2+}-dependent intercellular adhesion in staphylococcal biofilms. *Proc Natl Acad Sci USA* 110(3): E202–E211.
11. Krachler AM, Orth K (2013) Targeting the bacteria-host interface: Strategies in anti-adhesion therapy. *Virulence* 4(4):284–294.
12. Cozens D, Read RC (2012) Anti-adhesion methods as novel therapeutics for bacterial infections. *Expert Rev Anti Infect Ther* 10(12):1457–1468.
13. Brehm-Stecher BF, Johnson EA (2004) Single-cell microbiology: Tools, technologies, and applications. *Microbiol Mol Biol Rev* 68(3):538–559.
14. Dufrêne YF (2014) Atomic force microscopy in microbiology: New structural and functional insights into the microbial cell surface. *MBio* 5(4):e01363-14.
15. Xiao J, Dufrêne Y (2016) Optical and force nanoscopy in microbiology. *Nat Microbiol* 1(11):16186.
16. Bustanji Y, et al. (2003) Dynamics of the interaction between a fibronectin molecule and a living bacterium under mechanical force. *Proc Natl Acad Sci USA* 100(23): 13292–13297.
17. Lower SK, et al. (2010) A tactile response in *Staphylococcus aureus*. *Biophys J* 99(9): 2803–2811.
18. Lower SK, et al. (2011) Polymorphisms in fibronectin binding protein A of *Staphylococcus aureus* are associated with infection of cardiovascular devices. *Proc Natl Acad Sci USA* 108(45):18372–18377.
19. Herman P, et al. (2014) The binding force of the staphylococcal adhesin SdrG is remarkably strong. *Mol Microbiol* 93(2):356–368.
20. Herman-Bausier P, El-Kirat-Chatel S, Foster TJ, Geoghegan JA, Dufrêne YF (2015) *Staphylococcus aureus* fibronectin-binding protein A mediates cell-cell adhesion through low-affinity homophilic bonds. *MBio* 6(3):e00413-15.
21. Formosa-Dague C, Speziale P, Foster TJ, Geoghegan JA, Dufrêne YF (2016) Zinc-dependent mechanical properties of *Staphylococcus aureus* biofilm-forming surface protein SasG. *Proc Natl Acad Sci USA* 113(2):410–415.
22. Formosa-Dague C, et al. (2016) Sticky matrix: Adhesion mechanism of the staphylococcal polysaccharide intercellular adhesin. *ACS Nano* 10(3):3443–3452.
23. Formosa-Dague C, et al. (2016) Forces between *Staphylococcus aureus* and human skin. *Nanoscale Horiz* 1(4):298–303.
24. Barbu EM, Mackenzie C, Foster TJ, Höök M (2014) SdrC induces staphylococcal biofilm formation through a homophilic interaction. *Mol Microbiol* 94(1):172–185.
25. Barbu EM, et al. (2010) Beta-neurexin is a ligand for the *Staphylococcus aureus* MSCRAMM SdrC. *PLoS Pathog* 6(1):e1000726.
26. Boks NP, Busscher HJ, van der Mei HC, Norde W (2008) Bond-strengthening in staphylococcal adhesion to hydrophilic and hydrophobic surfaces using atomic force microscopy. *Langmuir* 24(22):12990–12994.
27. Oesterhelt F, et al. (2000) Unfolding pathways of individual bacteriorhodopsins. *Science* 288(5463):143–146.
28. Zhang Y, Sivasankar S, Nelson WJ, Chu S (2009) Resolving cadherin interactions and binding cooperativity at the single-molecule level. *Proc Natl Acad Sci USA* 106(1): 109–114.
29. Wu Y, et al. (2010) Cooperativity between *trans* and *cis* interactions in cadherin-mediated junction formation. *Proc Natl Acad Sci USA* 107(41):17592–17597.
30. Baumgartner W, et al. (2000) Cadherin interaction probed by atomic force microscopy. *Proc Natl Acad Sci USA* 97(8):4005–4010.
31. Alsteens D, et al. (2015) Imaging G protein-coupled receptors while quantifying their ligand-binding free-energy landscape. *Nat Methods* 12(9):845–851.
32. El-Kirat-Chatel S, Mil-Homens D, Beaussart A, Fialho AM, Dufrêne YF (2013) Single-molecule atomic force microscopy unravels the binding mechanism of a *Burkholderia cenocepacia* trimeric autotransporter adhesin. *Mol Microbiol* 89(4):649–659.
33. Fritz J, Katopodis AG, Kolbinger F, Anselmetti D (1998) Force-mediated kinetics of single P-selectin/ligand complexes observed by atomic force microscopy. *Proc Natl Acad Sci USA* 95(21):12283–12288.
34. Ponnuraj K, et al. (2003) A "dock, lock, and latch" structural model for a staphylococcal adhesin binding to fibrinogen. *Cell* 115(2):217–228.
35. Gross M, Cramton SE, Götz F, Peschel A (2001) Key role of teichoic acid net charge in *Staphylococcus aureus* colonization of artificial surfaces. *Infect Immun* 69(5): 3423–3426.
36. Houston P, Rowe SE, Pozzi C, Waters EM, O'Gara JP (2011) Essential role for the major autolysin in the fibronectin-binding protein-mediated *Staphylococcus aureus* biofilm phenotype. *Infect Immun* 79(3):1153–1165.
37. Schroeder K, et al. (2009) Molecular characterization of a novel *Staphylococcus aureus* surface protein (SasC) involved in cell aggregation and biofilm accumulation. *PLoS One* 4(10):e7567.
38. O'Brien L, et al. (2002) Multiple mechanisms for the activation of human platelet aggregation by *Staphylococcus aureus*: Roles for the clumping factors ClfA and ClfB, the serine-aspartate repeat protein SdrE and protein A. *Mol Microbiol* 44(4): 1033–1044.
39. Li MZ, Elledge SJ (2012) SLIC: A method for sequence- and ligation-independent cloning. *Methods Mol Biol* 852:51–59.
40. Holden MTG, et al. (2004) Complete genomes of two clinical *Staphylococcus aureus* strains: Evidence for the rapid evolution of virulence and drug resistance. *Proc Natl Acad Sci USA* 101(26):9786–9791.
41. Monk IR, Shah IM, Xu M, Tan M-W, Foster TJ (2012) Transforming the untransformable: Application of direct transformation to manipulate genetically *Staphylococcus aureus* and *Staphylococcus epidermidis*. *MBio* 3(2):e00277-11.
42. Kelley LA, Mezulis S, Yates CM, Wass MN, Sternberg MJE (2015) The Phyre2 web portal for protein modeling, prediction and analysis. *Nat Protoc* 10(6):845–858.
43. Chemical Computing Group (2017) Molecular Operating Environment (MOE) (Chem Comput Group, Montreal), Version 2013.08.
44. Trott O, Olson AJ (2010) AutoDock Vina: Improving the speed and accuracy of docking with a new scoring function, efficient optimization, and multithreading. *J Comput Chem* 31(2):455–461.
45. Pettersen EF, et al. (2004) UCSF Chimera—A visualization system for exploratory research and analysis. *J Comput Chem* 25(13):1605–1612.